Supplemental Information

Structural Basis of the pH-Dependent Assembly of a Botulinum Neurotoxin Complex

Tsutomu Matsui, Shenyan Gu, Kwok-ho Lam, Lester G. Carter, Andreas Rummel, Irimpan I. Mathews and Rongsheng Jin

Inventory of the Supplemental Information

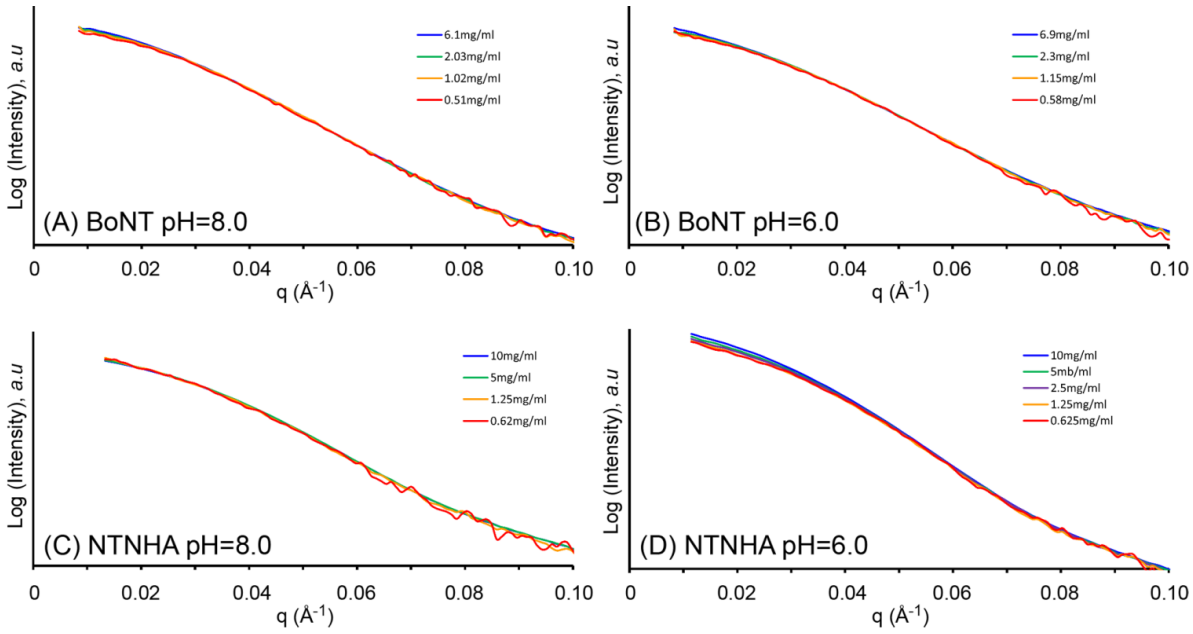

Fig. S1. SAXS profiles of BoNT/Ai and NTNHA-A at various examined concentrations.

A
(front view)
(side view)
pH=8.0
pH=6.0
pH=8.0 vs 6.0

B
(front view)
(side view)
pH=6.0
pH=8.0
pH=8.0 vs 6.0

Fig. S2. Reproducibility of rigid body refinements. (A) BoNT/Ai. The results from 10 independent runs were superimposed onto VHH and BoNT/Ai LC–H_N domains shown as molecular surface representations. H_C domains from each refinement were shown as ribbon representation. The average position of 10 runs was colored in black. Significant difference was not observed between pH = 6.0 and 8.0 (third column). The lack fragments and a flexible linker were not shown. (B) NTNHA-A. The 10 independent runs were superimposed onto NTNHA-A nLC–nH_N domains in the same way. Contrast to BoNT/Ai, the positioning of nH_C domain was well converged at each pH value and significant pH-dependence was observed. See Fig. S4 for more analyses on sensitivity of nH_C position to the scattering profile.

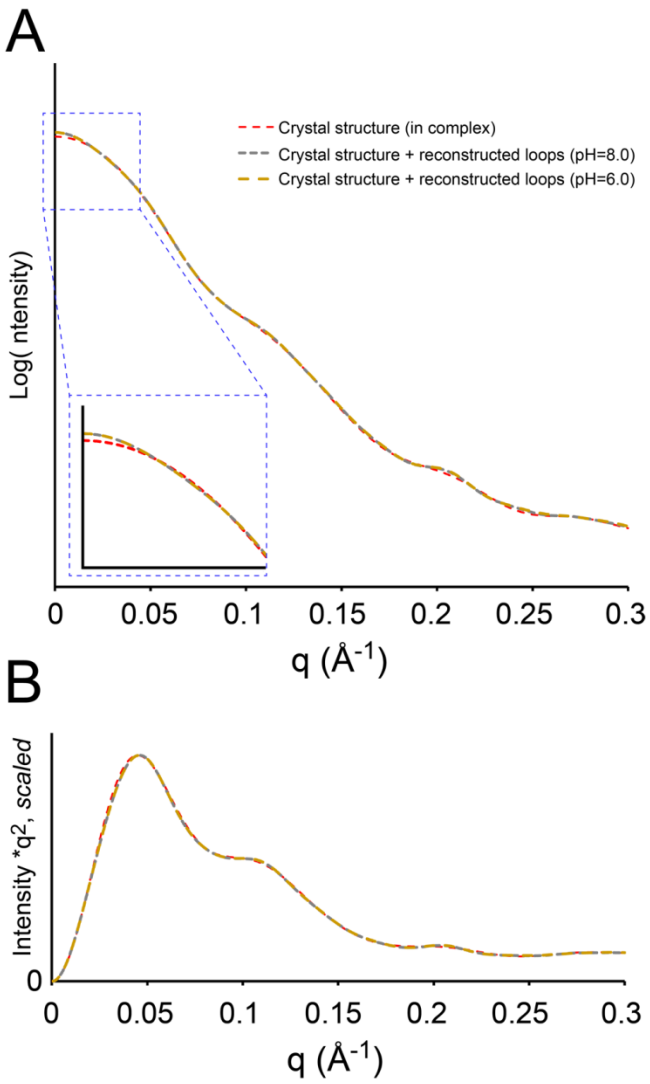

Fig. S3. The effect of reconstructed loops of NTNHA-A on its SAXS profile. (A) Both the long (Gly114–Ala148) and short (Try442–Asn450) loops reconstructed by SAXS-based rigid body refinements were replanted to the crystal structure of NTNHA-A, and the theoretical curve was then computed. There is no significant difference at the middle angle whereas subtle differences are exist at low and high angle parts. (B) Kratky plot derived from panel A. No significant difference is observed.

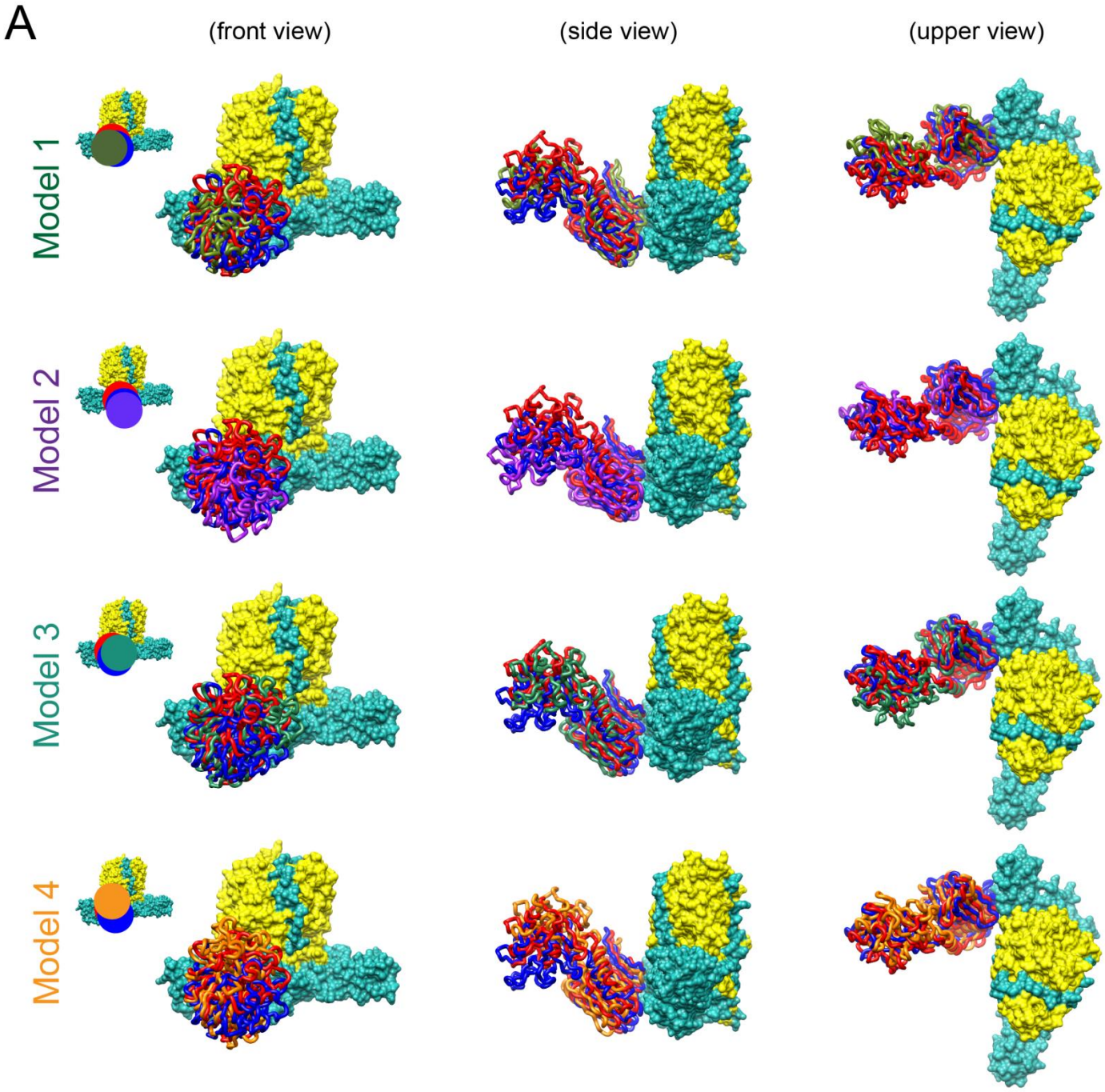
A
(front view)
(side view)
(upper view)
Model 1
Model 2
Model 3
Model 4

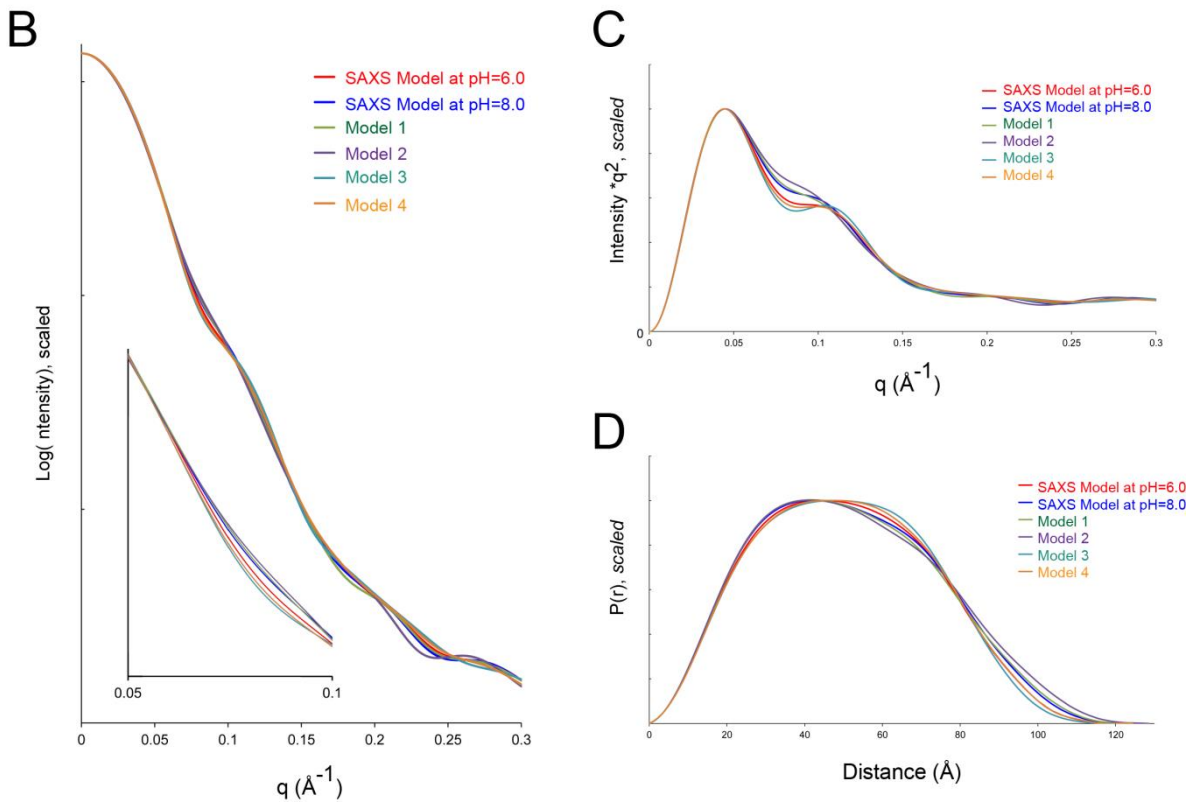

Fig. S4. Sensitivity of the nH_C domain positioning on the SAXS profile of NTNHA-A. (A) Four models with slightly different hinge motion of the nH_C domain were randomly generated based on the resultant models at pH = 6.0 (red) and 8.0 (blue). The disorder region simulated in Fig. S3 is not included. (B) Theoretical SAXS profiles of the four models. The profiles were scaled at I(0). Inset is a magnified view from q=0.05 to 0.10 $Å^{-1}$. (C) Theoretical Kratky plots, which were scaled at the peak height. The scattering profile at middle q angles is sensitive to a slight torsional motion of the nH_C domain and that is emphasized by Kratky plot. (C) Pair distance distributions P(r), which were scaled at the peak height. Such a slight motion can dramatically alter P(r) due to non-globular, elongated and asymmetric molecular shape of the nLC–nH_N and nH_C domains.

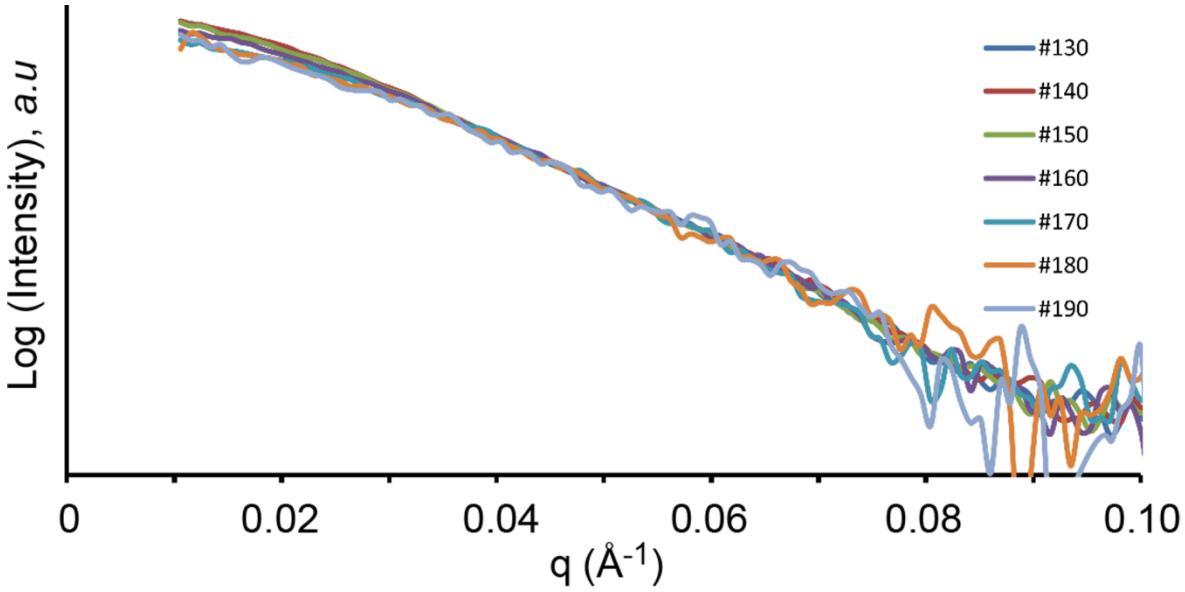

Fig. S5. Examples of FPLC-SAXS profiles of the M-PTC at different fractions. Concentration-dependent intermolecular interactions were observed.

Table S1: SAXS data collection and analysis.

Experimental Setup					
Beamline	SSRL BL4-2				
Type of monocromter	Si(111)				
Defining Slits size (mm)	0.3(H) x 0.3 (V)				
Beam energy (keV)	11				
Beam current	300 mA with 5 min top-off mode				
Sample-Detector Distance (m)	1.7				
Detector	Rayonix MX225-HE				
Pixel binning	8x8				
Pixel size (mm)	292				
Exposure time (sec)	1				
Type of sample Cell	Quatz capillary (Diameter=1.5mm)				
Sample volumn per data set (ml)	30				
Rate of oscillation (ml/sec)	2				
Measurement repeats	15				
Temperature (K)	283				
Data analysis	BoNT/Ai	BoNT/Ai	NTNHA-A	NTNHA-A	M-PTC
pH	pH=8	pH=6	pH=8	pH=6	pH=6
Type of SAXS experiment	Equilibrium	Equilibrium	Equilibrium	Equilibrium	FPLC
Max protein concentration (mg/ml)	6.1	6.9	10	10	N.A.
Min protein concentration (mg/ml)	0.51	0.58	0.63	0.63	N.A.
Rg (qRg<1.3)	43.3	43.7	39.7	39.5	51.2
SD	0.24	0.22	0.06	0.26	0.55
Rg (real)	44.7	44.9	39.9	40.3	52.2
SD	0.10	0.06	0.02	0.06	0.14
Rg (reciprocal)	44.6	44.8	39.9	40.3	52.1
Dmax	150	153	127.5	131	167.5
Molecular weight estimation					
SAXS MoW, q<0.3 (kDa)	158.8	152.7	139.5	143.3	343.6
based on water scattering (kDa)	122.7	118.7	101.2	105.1	N.A.
Modeling	BoNT/Ai	BoNT/Ai	NTNHA-A	NTNHA-A	M-PTC
pH	pH=8	pH=6	pH=8	pH=6	pH=6
Methods	Rigid body	Rigid body	Rigid body	Rigid body	ab initio
Program	CORAL	CORAL	CORAL	CORAL	GASBOR
qmin	0.0177	0.0177	0.0152	0.0152	0.0171
qmax	0.3	0.3	0.3	0.3	0.3
Chi square (SAXS model)	2.21	2.49	2.11	2.31	N/A
Chi square (Crystal Structure)	3.84	4.37	10.98	15.04	3.19*
BIOISIS ID (http://www.bioisis.net)	BONT8P	BONT6P	NTNH8P	NTNH6P	MPTC6P
Crystal Structure*	BoNT/A	BoNT/Ai		NTNHA-A	M-PTC
pH	7	6		6	6
PDB ID	3BTA	3V0A		3V0A	3V0A
Conformation	Free form	In complex		In Complex	Complex
Rg**	43.4	41.1		38.4	46.4
Dmax**	156.2	144.1		125.4	179
Full-length (aa)	1413**	1413**		1193	2606**
Disorder residues (aa)	18	18		44	62
Disorder residues (%)	1.27	1.27		3.69	2.38
Molecular Weight	159.2	159.2		131.8	278.1

*VHH with BoNT/Ai is taken into account. **All side chains are taken into account.

Table S2: Summary of rigid body refinement by program CORAL.

	Original position (center of domain)			Refined position (center of domain)			Mobility btw domain centers. (Å)	Rotation and translation matrix			
	x	y	z	x	y	z					
BoNT/Ai (pH=6.0)	2.27	39.56	55.26	-4.09	53.17	54.58	15.03	0.965261 -0.261264 -0.00364706	0.182831 0.685324 -0.704914	0.186668 0.679759 0.709283	-23.8271 -10.9193 43.2771
BoNT/Ai (pH=8.0)	2.27	39.56	55.26	-5.05	54.35	53.41	16.61	0.973669 -0.227469 -0.015022	0.166944 0.756365 -0.632489	0.155234 0.613327 0.774424	-22.4419 -8.94977 35.6654
NTNHA-A (pH=8.0)	-2.05	-1.68	-26.41	-2.76	-5.26	-25.58	3.74	0.895671 -0.120207 0.428163	-0.121028 0.860551 0.494777	-0.427931 -0.494977 0.756222	-12.4249 -17.1319 -3.89463
NTNHA-A (pH=6.0)	-2.05	-1.68	-26.41	-2.18	-1.03	-22.30	4.17	0.850463 -0.0762804 0.520475	-0.343842 0.668189 0.65977	-0.398103 -0.740071 0.542041	-11.5323 -19.6154 -5.80595